AC

C.E. SACLAY
DSM

SERVICE DE PHYSIQUE DES PARTICULES

CERN LIBRARIES, GENEVA
SCAN-9601314

W9607

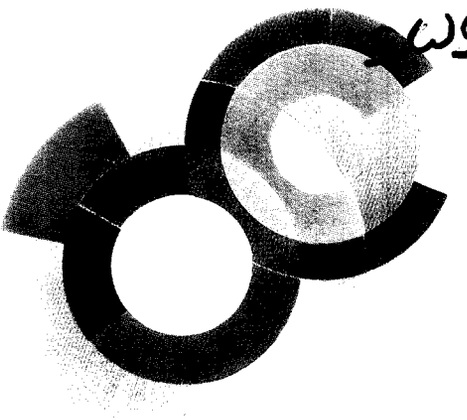

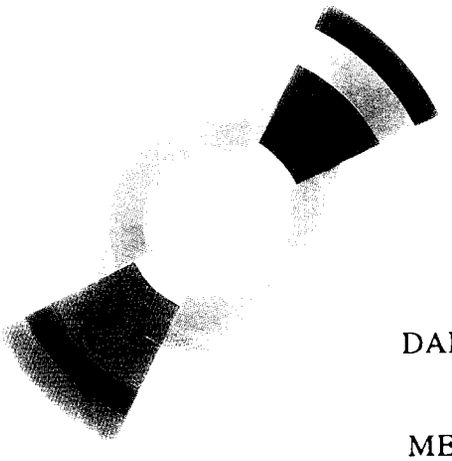

DAPNIA/SPP 96-03 January 1996

MEASUREMENT OF THE TOTAL CROSS SECTION DIFFERENCE $\Delta\sigma_L$ IN np TRANSMISSION AT 1.19, 2.49 AND 3.65 GeV.

F. Lehar, De Lesquen et al.,

DAPNIA

Submitted to Zeitschrift für Physik C

Le DAPNIA (**Dé**partement d'**A**strophysique, de physique des **P**articules, de physique **N**ucléaire et de l'**I**nstrumentation **A**ssociée) regroupe les activités du Service d'Astrophysique (SAp), du Département de Physique des Particules Elémentaires (DPhPE) et du Département de Physique Nucléaire (DPhN).

Adresse : DAPNIA, Bâtiment 141
CEA Saclay
F - 91191 Gif-sur-Yvette Cedex

MEASUREMENT OF THE TOTAL CROSS SECTION DIFFERENCE $\Delta\sigma_L$ IN np TRANSMISSION AT 1.19, 2.49 AND 3.65 GeV

B.P. Adiasevich[4], V.G. Antonenko[4], S.A. Averichev[1], L.S. Azhgirey[2], J. Ball[5], N.A. Bazhanov[6], B. Benda[3], N.S. Borisov[2], Yu.T. Borzunov[1], E.I. Bunyatova[2], V.F. Burinov[2], E.V. Chernykh[1], S.A. Dolgii[1], G. Durand[3], A.P. Dzyubak[7], A.N. Fedorov[8], V.V. Fimushkin[1], J.M. Fontaine[5], V.V. Glagolev[1], L.B. Golovanov[1], D.P. Grosnick[9], G.M. Gurevich[10], D.A. Hill[9], A.V. Karpunin[1], T.E. Kasprzyk[9], B.A. Khachaturov[2], A.D. Kirillov[1], N.I. Kochelev[11], A.D. Kovalenko[1], A.I. Kovalev[6], M.V. Kulikov[1], V.P. Ladygin[1], A.B. Lazarev[2], F. Lehar[3], A. de Lesquen[3], M.Yu. Liburg [1], D. Lopiano[9], A.A. Lukhanin[7], P.K. Maniakov[1], V.N. Matafonov[2], E.A. Matyushevsky[1], G. Mgebrishvili[4], S.V. Mironov[1], A.B. Neganov[2], G.P. Nikolaevsky[1], A.A. Nomofilov[1], Yu.K. Pilipenko[1], I.L. Pisarev[2], N.M. Piskunov[1], Yu.A. Plis[2], Yu.P. Polunin[4], V.V. Polyakov[6], A.N. Prokofiev[6], D.A. Ronzhin[2], P.A. Rukoyatkin[1], J.L. Sans[5], V.I. Sharov[1], S.N. Shilov[2], Yu.A. Shishov[1], V.B. Shutov[1], P.V. Sorokin[7], H.M. Spinka[9], A.Yu. Starikov[1], G.D. Stoletov[2], E.A. Strokovsky[1], L.N. Strunov[1], A.L. Svetov[1], V.V. Teterin[2], S.V. Topalov[10], V.Yu. Trautman[6], A.P. Tsvinev[1], Yu.A. Usov[2], V.V. Vikhrov[6], V.I. Volkov[1], A.A. Yershov[12], V.P. Yershov[1], S.A. Zaporozhets[1], A.A. Zhdanov[6],

Present address :

1) Laboratory of High Energies, JINR, 141980 Dubna, Moscow Region, Russia,
2) Laboratory of Nuclear Problems, JINR, 141980 Dubna, Moscow Region, Russia,
3) CEA-DAPNIA, CE Saclay, 91191 Gif sur Yvette Cedex, France,
4) I.V.Kurchatov Institute of Atomic Energy, Kurchatova str. 46, 123182 Moscow, Russia,
5) Laboratoire National SATURNE, CNRS/IN2P3 and CEA/DSM, CE Saclay, 91191 Gif sur Yvette Cedex, France,
6) Petersburg Nuclear Physics Institute, 188350, Gatchina, Russia,
7) Kharkov Institute of Physics and Technology, Academicheskaya str. 1, 310108 Kharkov, Ukraine,
8) Laboratory of Particle Physics, JINR, 141980 Dubna, Moscow Region, Russia
9) ANL-HEP, 9700 South Cass Avenue, Argonne, IL 60439, USA,
10) Institute for Nuclear Research, Russian Academy of Sciences, 60th October Anniversary Prospect 7A, 117312 Moscow, Russia,
11) Laboratory of Theoretical Physics, JINR, 141980 Dubna, Moscow Region, Russia.
12) Institute of Nuclear Physics, Moscow State University, 119899 Moscow, Russia,

Submitted to Zeitschrift für Physik C

ABSTRACT

Results of the total cross section difference $\Delta\sigma_L$ in a np transmission experiment at 1.19, 2.49 and 3.65 GeV incident neutron beam kinetic energies are presented. Measurements were performed at the Synchrophasotron of the Laboratory of High Energies of the Joint Institute for Nuclear Research in Dubna. Results were obtained with a polarized beam of free quasi-monochromatic neutrons passing through the new Dubna frozen spin proton target. The beam and target polarizations were oriented longitudinally. The present results were obtained at the highest energies of free polarized neutrons that can be reached at present. They extend the energy range of existing results from PSI, LAMPF and Saclay measured between 0.066 and 1.10 GeV. The new results are compared with $\Delta\sigma_L(pn)$ data determined as a difference between $\Delta\sigma_L(pd)$ and $\Delta\sigma_L(pp)$ ANL-ZGS measurements. The values of $\Delta\sigma_L$ for the isospin state I=0 were deduced using known pp data.

1. INTRODUCTION

The aim of this paper is to present new results of the neutron-proton total cross section difference $\Delta\sigma_L$ measured with a quasi-monochromatic polarized neutron beam and a polarized proton target. Results were obtained at the central values of 1.19, 2.49 and 3.65 GeV neutron beam kinetic energies. The free polarized neutron beam was produced by break-up of polarized deuterons accelerated by the Synchrophasotron of the Laboratory of High Energies (LHE) of the Joint Institute for Nuclear Research (JINR) in Dubna. This accelerator provides the highest energy polarized neutron beam, which can be reached now [1]. The present experiment is the first one of series where the new Dubna polarized proton target was used.

The nucleon-nucleon (NN) total cross section differences $\Delta\sigma_T$ and $\Delta\sigma_L$ together with the spin-independent total cross section σ_{0tot} are integral quantities linearly related with three non-vanishing imaginary parts of the NN forward scattering amplitudes via optical theorems. They are used for absolute normalization in any theoretical or phenomenological analysis. The observable σ_{0tot} has been measured during the last fifty years from 10^{-2} eV up to thousands of TeV. A surprising behaviour in the energy dependence of σ_{0tot} has been observed and remains unexplained. The measurements of spin-dependent total cross section are rare due to a lack of polarized beams and targets. All three observables are measured in pure inclusive transmission experiments and need very high stability of detectors.

The total cross section differences for pp scattering were first measured at the ANL-ZGS and then in a few other laboratories: TRIUMF, PSI, LAMPF and SATURNE II. Results cover the energy range from 0.2 to 12 GeV. Another point was measured at 200 GeV at FERMILAB for proton-proton and antiproton-proton interactions. Measurements with incident charged particles need a different experimental set-up than neutron-proton experiments due to the contribution of electromagnetic interactions. Existing results are discussed in [2] and in references therein. The isospin $I = 1$ data are also needed in order to deduce the isospin $I = 0$ quantities from np measurements.

Neutron-proton observables, $\Delta\sigma_T$ and $\Delta\sigma_L$ using free polarized neutrons, were first obtained in 1987 at SATURNE II yielding four points with relatively large errors [3]. These results have been completed by new accurate measurements at 9 to 10 energies, between 0.31 and 1.1 GeV for each observable [4,5]. The Saclay results were soon followed by PSI measurements [6] in the energy region from 0.14 to 0.59 GeV with a continuous neutron energy spectrum [7]. The $\Delta\sigma_T(np)$ or $\Delta\sigma_L(np)$ data were collected simultaneously over the entire energy range. The PSI and Saclay sets

allowed to deduce imaginary parts of np and $I = 0$ spin-dependent forward scattering amplitudes from 0.14 to 1.1 GeV [2,5].

The observable $\Delta\sigma_L(np)$ has also been measured at five energies at LAMPF [8]. The measurements were done with a quasi-monoenergetic polarized neutron beam produced in $pd \Rightarrow n+X$ scattering of longitudinally polarized protons. Large neutron counter hodoscopes have to be used because of the small neutron beam intensity.

In addition, at low energies, the observable $\Delta\sigma_L(np)$ at 66 MeV was measured at the PSI preaccelerator [9], $\Delta\sigma_T(np)$ was determined at 9 energies between 3.8 and 11.6 MeV in TUNL [10,11] and at 16.2 MeV in Prague [12].

In fact, for the first time $\Delta\sigma_L(pn)$ results were deduced in 1981 from the $\Delta\sigma_L(pd)$ and $\Delta\sigma_L(pp)$ measurement at the ANL-ZGS [13]. Taking a simple difference between pd and pp results, corrected only for beam and target polarizations and for Coulomb-nuclear rescattering including deuteron break-up, yields data in fairly good agreement with free np data (see Section 6). Let us note that any correction for Glauber-type rescattering including 3-body state final interactions [14] provides a disagreement [2].

In Section 2 we shortly describe the phenomenology of the experiment. Section 3 treats the LHE polarized deuteron and neutron beams and beam polarization measurements. In Section 4 the new Dubna polarized proton target is described. The experimental set-up for the $\Delta\sigma_L(np)$ measurements with associated electronics are described in Section 5. The data analysis and systematic errors are treated in Section 6. Results and discussions are presented in Section 7.

2. TOTAL CROSS SECTION DIFFERENCES

Throughout this paper we use the nucleon-nucleon formalism and the four-spin notation of observables developed in ref.[15].

The general expression of the total cross section for a polarized nucleon beam transmitted through a polarized proton target (PPT), with arbitrary directions of beam and target polarizations, was first deduced in refs[16,17]. Taking into account fundamental conservation laws, it is written in ref.[15] in the form :

$$\sigma_{tot} = \sigma_{0tot} + \sigma_{1tot}(\vec{P}_B, \vec{P}_T) + \sigma_{2tot}(\vec{P}_B, \vec{k})(\vec{P}_T, \vec{k}), \tag{2.1}$$

where $\vec{P}_B$ and $\vec{P}_T$ are the beam and target polarization vectors (more exactly pseudovectors), and $\vec{k}$ is the unit vector in the incident beam direction. The term σ_{0tot} is the spin-independent total cross section, σ_{1tot} and σ_{2tot} are the spin dependent contributions. They are related to the forward scattering invariant amplitudes via

optical theorems [15] :

$$\sigma_{0tot} = (2\pi/K)Im[a(0) + b(0)], \tag{2.2}$$

$$\sigma_{1tot} = (2\pi/K)Im[c(0) + d(0)], \tag{2.3}$$

$$\sigma_{2tot} = -(4\pi/K)Im[d(0)], \tag{2.4}$$

where K is the wave number in the CM system.

The total cross sections σ_{tot} and σ_{0tot} are positive definite quantities. The spin-dependent contributions σ_{1tot} and σ_{2tot} are related to measurable quantities $\Delta\sigma_T$ and $\Delta\sigma_L$ by :

$$-\Delta\sigma_T = 2\sigma_{1tot}, \tag{2.5}$$

$$-\Delta\sigma_L = 2(\sigma_{1tot} + \sigma_{2tot}). \tag{2.6}$$

The negative signs for $\Delta\sigma_T$ and $\Delta\sigma_L$ in Eqs (2.5) and (2.6) correspond to the usual, although unjustified, convention in the literature. The total cross section differences are measured with either parallel or antiparallel beam and target polarization directions. Polarization vectors are transversally oriented with respect to $\vec{k}$ for $\Delta\sigma_T$ measurements and longitudinaly oriented for $\Delta\sigma_L$ experiments.

The total cross section differences $\Delta\sigma_T$ and $\Delta\sigma_L$ are deduced from four total cross section measurements, respectively. General expressions for $\Delta\sigma_T$ are given in ref.[18]; here we give relations for $\Delta\sigma_L$:

$$\sigma(\rightrightarrows) = \sigma_{0tot} + |P_B^+ P_T^+|(\sigma_{1tot} + \sigma_{2tot}), \tag{2.7a}$$

$$\sigma(\leftrightarrows) = \sigma_{0tot} - |P_B^- P_T^+|(\sigma_{1tot} + \sigma_{2tot}), \tag{2.7b}$$

$$\sigma(\rightleftarrows) = \sigma_{0tot} - |P_B^+ P_T^-|(\sigma_{1tot} + \sigma_{2tot}), \tag{2.7c}$$

$$\sigma(\leftleftarrows) = \sigma_{0tot} + |P_B^- P_T^-|(\sigma_{1tot} + \sigma_{2tot}). \tag{2.7d}$$

Since the beam polarization direction at the Synchrophasotron could be reversed at every cycle of the accelerator, it is preferable to calculate $\Delta\sigma_L$ from pairs of $|P_B^+|$ and $|P_B^-|$ measurements with the same target polarization. Values of $|P_T^+|$ and $|P_T^-|$ are well known as a function of time. The spin-independent term drops out when taking the difference, and one obtains :

$$-\Delta\sigma_L(P_T^+) = 2(\sigma_{1tot} + \sigma_{2tot})^+ = \frac{2[\sigma(\rightrightarrows) - \sigma(\leftrightarrows)]}{(|P_B^+| + |P_B^-|)|P_T^+|}, \tag{2.8a}$$

and

$$-\Delta\sigma_L(P_T^-) = 2(\sigma_{1tot} + \sigma_{2tot})^- = \frac{2[\sigma(\leftleftarrows) - \sigma(\rightleftarrows)]}{(|P_B^+| + |P_B^-|)|P_T^-|}, \tag{2.8b}$$

with beam and target polarized along $\vec{k}$. The asymmetry, proportional to the arithmetic average

$$P_B = |P_B| = \frac{1}{2}(|P_B^+| + |P_B^-|) \tag{2.9}$$

is continuously measured by beam polarimeters. One can see that an unpolarized beam is not necessary for $\Delta\sigma_{L,T}$ measurements.

Possible effects of a counter misalignment and perpendicular components in the beam (or target) polarization cancel out, giving the final results as a simple (unweighted) average

$$\Delta\sigma_L = \frac{1}{2}[\Delta\sigma_L(P_T^+) + \Delta\sigma_L(P_T^-)]. \tag{2.10}$$

Putting Eqs(2.8a) and (2.8b) into Eq.(2.10) we have

$$\Delta\sigma_L = \frac{1}{|P_B^+| + |P_B^-|}\left(\frac{\sigma(\rightrightarrows) - \sigma(\leftrightarrows)}{|P_T^+|} + \frac{\sigma(\leftrightarrows) - \sigma(\rightleftarrows)}{|P_T^-|}\right). \tag{2.11}$$

More details are given in refs[4,18].

3. POLARIZED BEAM

Polarized neutrons and protons were produced by break-up of accelerated vector-polarized deuterons [1] on a target of 17 cm beryllium and 6 cm of carbon. The kinetic energy of accelerated deuteron decreases of 3 MeV by passage in air and then of 17 MeV by absorption in the half of of the target thickness. The total losses of (20 $\pm$ 17)MeV are practically the same at all measured energies and must be subtracted from the nominal accelerator values. The neutron mean energy is then one half of the deuteron energy in the center of the production target. The neutron momentum distribution in the forward break-up reaction, due to the Fermi motion of the nucleons in accelerated deuterons has a gaussian-like shape with FWHM $\sim$ 5% of neutron momentum.

The production target was positioned close to one focal point of the deuteron beam line. Protons and deuterons were removed from the neutron beam by a bending magnet. The deuteron beam intensity was continuously monitored by two calibrated ionization chambers in front of the target. Neutrons were collimated by 6 m iron and brass in a path of 7 m upstream from the transmission set-up. The neutron angular divergence was $\sim$ 1.5 mrad. The collimators and efficient shielding of the experimental area decreased the low energy tail of the neutron spectrum to about 1%.

The neutron beam spot at the PPT was 28 mm in diameter. This spot was monitored using charge exchange particles produced in a radiator of a proportional

chamber downstream from the PPT. The number of neutrons was determined in dedicated measurements by an activation method. The deuteron beam intensities and corresponding neutron fluxes at the PPT, averaged over the data acquisition, are listed in Table 1.

Table 1

Averaged deuteron beam intensities and neutron fluxes at three energies

$T_{kin}(d)$ (GeV) accererator	$T_{kin}(d)$ (GeV) target center	$T_{kin}(n)$ (GeV) mean	Deuterons per spill	Neutrons per spill (PPT)
2.40	2.38	1.19	5.3×10^8	2.7×10^4
5.00	4.98	2.49	6.1×10^8	2.0×10^5
7.32	7.30	3.65	6.4×10^8	4.7×10^5

The neutron intensity decreases with decreasing neutron momentum $p_{lab}(n)$ since the neutron emission solid angle increases as a function of $1/[p_{lab}(n)]^2$. From Table 1 follows that the intensity decreases more rapidly due to a degradation of the beam extraction efficiency at lower energies.

The repetition time of the Synchrophasotron was 8 to 10 sec, depending on energy, and the spill length was typically 0.5 sec. The deuteron beam polarization direction was flipped every spill of the accelerator.

The polarization of incident deuterons $\vec{P}_B(d)$ was oriented along the vertical axis and the polarization of the produced neutrons $\vec{P}_B(n)$ had the same direction. The neutron polarization was rotated to the longitudinal direction by a spin rotation dipole with the maximum horizontal field integral of 2.7 Tm. The spin rotator was positioned in front of the PPT and removed a considerable fraction of the protons produced in collimators. The beam line allowed to extract the low intensity deuteron beam towards the experimental area and check the beam alignment and bending of deuterons in the spin rotator. This procedure checks the signs of the $\Delta\sigma_L$ results.

The absolute polarization of deuterons was deduced from the asymmetry measurement of $dp \Rightarrow dp$ elastic scattering. For this reason the deuteron beam was periodically deviated into another beam line towards the two-arm magnetic spectrometer ALPHA [19]. The deuteron beam momentum was set to 3.0 GeV/c where the analyzing power is well known from the SATURNE II measurements [20]. Deuterons were scattered in the liquid hydrogen target, forward deuterons and recoil protons were detected in two pairs of kinematically conjugate arms at $\theta_{lab}(d) = 7.45^o$. This angle is close to a maximum vector analyzing power. The magnetic analysis of forward

deuterons removed inelastic events [19]. The measurement provided the $P_B(d)$ value, directly related to the neutron beam polarization $P_B(n)$. The results yields the mean value for "up" and "down" neutron beam polarization $|P_B(n)| = 0.535 \pm 0.009$.

No depolarizing resonances of the internal deuteron beam in the synchrophasotron exist up to the highest accelerator energy. This has been determined over the entire energy range [19] using a beam decceleration method described in ref.[21]. Consequently, it was sufficient to determine the deuteron beam polarization at one energy only.

A direct absolute measurement of the neutron beam polarization has not be performed during the run. The $P_B(n)$ could be determined e.g. by a comparison of the beam and target analyzing powers, $A_{oono}(np)$ and $A_{ooon}(np)$, respectively [15], assuming that the target polarization P_T is known [22].

The stability of the $P_B(d)$ value was continuously monitored by another beam polarimeter [23], measuring quasielastic scattering of bounded protons in accelerated deuterons on a CH_2 target. This polarimeter consists of two pairs of arms, each of them equipped with two scintillation counters. Both pairs of arms were positioned at $pp \Rightarrow pp$ kinematically conjugate angles and measured the left-right asymmetry $\epsilon(pp)$. The angle was close to the forward maximum of the pp elastic scattering analyzing power A_{oono}. The measurement showed the excellent stability of $\epsilon(pp)$ during data taking. The dispersion of $\Delta\epsilon(pp)$ was smaller than $\pm$ 0.005 for each energy. This was deduced from the χ^2 value fitting results of indivivual runs to a constant. The mean values of $\epsilon(pp)$ at four proton energies (including data at the deuteron beam momentum 3 GeV/c) are given in Table 2.

Table 2

Mean values of the quasielastic pp asymmetry at four proton energies

$T_{kin}(p)$ (GeV)	$p_{lab}(p)$ (GeV/c)	θ_{lab} (deg)	θ_{CM} (deg)	$\epsilon(pp)$
0.83	1.50	14	33.3	0.246 $\pm$ 0.016
1.20	1.92	14	35.4	0.2214 $\pm$ 0.0015
2.50	3.31	8	24.2	0.1434 $\pm$ 0.0015
3.66	4.50	8	27.1	0.0807 $\pm$ 0.0020

4. POLARIZED PROTON TARGET

The Dubna target for the present experiment contains main parts of the Saclay-Argonne frozen spin proton polarized target, used initially in the E704 experiment at

FERMILAB (USA) [24,25]. The target has been reassembled and upgraded adding the missing parts for the purposes of the Dubna physics program. With respect to the FERMILAB experiment a concept of a "movable polarized target" (MPT) has been applied [26]. It consists in a transportability of the target from one experimental area to another. All the major parts of the target assembly located close to the beam line were mounted on two separate decks, which can be moved as units in and out of the beam, even when the target is polarized.

The largest of the two movable decks contains the $^3He/^4He$ horizontal dilution refrigerator mounted on a 1.5 ton concrete cube, a 30 ℓ service helium dewar of the refrigerator, a 1000 ℓ supply helium dewar, the ^3He pumping system, the NMR system and a microwave generator. These last two items are used for dynamic nuclear polarization measurement and build-up. The quality of the vibrational insulation was demonstrated by the fact that it was possible to work in the frozen polarization mode at a working temperature of 50 mK without any additional thermal load to the refrigerator, and only a negligible phonic noise on the NMR coils was observed.

A polarizing superconducting solenoid, its 300 ℓ service helium dewar and power supplies are mounted on the smaller deck. For easier operation and for a free access to detectors, the target equipment not mounted on the decks is placed outside of the radiation controlled area.

Remote control of the entire operation of the MPT consisted of the ^3He and ^4He control panels, an interlock system, and controls for the NMR and microwave systems. A new powerful two-arm cleaning system for ^3He was built (warm silicagel traps and charcoal traps cooled by liquid nitrogen).

The target material used in the experiment was 1,2-propanediol $C_3H_6(OH)_2$ with a paramagnetic Cr^V impurity, having a spin concentration of $1.5\text{x}10^{20} cm^{-3}$ (ref.[27]). The propanediol beads were loaded in a hydrogen-free container placed inside the dilution refrigerator. The PPT contains $(8.93 \pm 0.27).10^{23}/cm^{-2}$ polarized hydrogen atoms. The target characteristics at the room temperature and at the temperature of liquid nitrogen (70 K) are given in Table 3.

Table 3

Characteristics of the MPT.

Target length (mm) [20°C]	Target diameter (mm) [20°C]	Container volume (cm^3) [20°C]	Sample weight (g) [70 K]	Filling factor
200.0 ± 0.1	30.0 ± 0.1	141.37 ± 0.95	95.5 ± 0.3	0.67

The target polarization measurements were carried out using a computer controlled NMR system. Maximum values of proton polarization obtained were 0.842 and -0.906 for positive and negative polarizations, respectively. The difference of microwave frequencies corresponding to polarization maxima was measured to be 340 MHz. The duration of one continuous run at a given sign of target polarization was about 12 hours. The polarization degradation during this period was insignificant since the nuclear spin relaxation time in the frozen spin mode (at a temperature 50 mK and magnetic field 2.69 Tesla) was over 1000 hours.

For further experiments a transverse polarization of protons (and deuterons) is foreseen and a set of transverse holding coils is under construction.

5. TRANSMISSION DETECTORS SET-UP AND ELECTRONICS

The experimental set-up is shown in Fig. 1. The hardware used was described in detail in refs[2,3]; here we give only the most important items. The setup consisted of 5 independent units, two of them are used as beam monitors (S_i), and the three remaining ones as transmission detectors (T_j). The units were of similar design and the electronics were identical. We can discuss only one pair of S_i and T_j (i = 1,2 and j = 1,2,3). Each unit consisted of a CH_2 converter placed behind a large veto scintillation counter S3A (T3A). Charged particles emitted forward were detected by two counters S1 and S2 (T1 and T2) in coincidence. The monitor converters and S1,2 counters were 30 mm in diameter and the corresponding elements of the transmission detectors were 90 mm. It has been measured that with increasing radiator thickness, the detector efficiency first increases, reaches a broad maximum at about 60 - 80 mm, and then starts to decrease slowly. For this reason the thickness of all converters was set to 60 mm. The transmission detectors, each close to the other were positioned 6 meters downstream from the target center.

The electronics of one S unit is shown in Fig. 2.

The following rates were recorded for each spill of the accelerator :

$$
\begin{aligned}
S13 &= (S1.\overline{S3A}).(S2.\overline{S3A}), \\
T13 &= (T1.\overline{T3A}).(T2.\overline{T3A}), \\
S1A &= (S1.\overline{S3A}), \\
S2A &= (S2.\overline{T3A}), \\
T1A &= (T1.\overline{T3A}), \\
T2A &= (T2.\overline{T3A}),
\end{aligned}
$$

as well as accidental coincidences:

$$S13F = S1A.S2A(delayed),$$
$$T13F = T1A.T2A(delayed)$$

and single counts in each of the six counters. These data were recorded for each unit S_i and T_j by scalers, and were read by the computer after the end of every spill. A necessary statistics for this type of experiment can only be obtained from scalers rates, rather then individual events written on tape.

6. DATA ACQUISITION AND EXPERIMENTAL ERRORS

If N_{in} is the number of neutrons incident on the target and N_{out} the number of neutrons transmitted in a counter array of solid angle Ω, then the total cross section is :

$$N_{out} = N_{in} exp[-\sigma(\Omega) n_H x], \tag{6.1}$$

where n_H is the number of oriented hydrogen atoms per cm^3 and x is the target thickness. $\sigma(\Omega)$ depends on the polarizations $P_B^{\pm}$ and $P_T^{\pm}$ as shown in Eqs.(2.7a,b,c,d). If one sums over the events taken with fixed target polarization P_T^+ and P_T^- as shown in Eqs.(2.7a,b,c,d) and using Eq.(2.8a) or (2.8b), the ratio of the measurements with the beam polarization P_B from Eq.(2.9) becomes :

$$R^{\pm} = \frac{(N_{out}/N_{in})^-}{(N_{out}/N_{in})^+} = exp[\Delta\sigma(\Omega) P_B P_T^{\pm} n_H x] \tag{6.2}$$

for either target polarization $P_T^{\pm}$.

Because $N_{out} = T/\eta(T)$ and $N_{in} = S/\eta(S)$ where $T = T13 - T13F$ ($S = S13 - S13F$) is the number of neutrons seen in the T (S) detector and $\eta(T)$ ($\eta(S)$) its efficiency, we get:

$$R(P_T^{\pm}) = \frac{[T/S](P_B^-)}{[T/S](P_B^+)} \tag{6.3}$$

and

$$\Delta\sigma_L(\Omega, P_T^{\pm}) = \frac{1}{P_B.P_T^{\pm}.n_H.x} lnR(P_T^{\pm}). \tag{6.4}$$

As can be seen from Eq.(6.4) the statistical error of $\Delta\sigma_L$ decreases linearly with increasing x. Uncertainties in a determination of P_B, P_T and $n_H.x$ are normalization errors which move all results up or down independent of energy. We estimate the relative errors $\Delta P_B/P_B = \pm 2.3\%$, $\Delta P_T/P_T = \pm 3.0\%$ and $\Delta(n_H.x)/(n_H.x) = 3.1\%$, including the uncertainty of the filling factor and a possible error of the target temperature measurement. The spin rotator field setting and its inhomogeneity may provide

an additional systematic error of $\pm 1.1\%$, which is constant during measurements at one energy only.

All the formulae in Section 2 were deduced for a pure polarized hydrogen target. The presence of carbon and oxygen in the PPT beads add terms $\sigma_{tot}(C)$ in Eqs(2.7). These terms are spin-independent, since ^{12}C has no spin and therefore its contribution drops out in differences (2.8). The same occurs for ^{16}O and ^{4}He in the target. However, there are negligibly small contributions from ^{13}C and ^{3}He, which may be slightly polarized. This uncertainty was estimated to be 0.5%. No spin-dependent effect from the teflon container for the Saclay target [28] in working conditions has been observed. The ratio of polarized hydrogen to other target nuclei depends on the target material, and is fairly independent of target size.

Since a transmission spin effect manifests itself in the presence of polarized beam and target only, no contribution to $\Delta\sigma$ occurs if some beam neutrons miss the PPT. This will increase the spin-independent term, subtracted in differences.

The extrapolation of $\Delta\sigma_L(\Omega)$ towards zero solid angle gives $\Delta\sigma_L$. The maximal solid angle subtended by each of the three T detectors from the center of the MPT was about $\Omega_{lab} = 3.44 \times 10^{-4}$ sr i.e. $\theta_{lab} = 0.6^o$. The laboratory angle corresponds to $\theta_{CM} = 1.54^o$, 1.83^o and 2.06^o at 1.20, 2.50 and 3.66 GeV, respectively. The angles are small enough that the extrapolation of results towards $\Omega = 0$ is not necessary. In our energy range the difference between the measured value and the value extrapolated to $\Omega = 0$ is expected to be smaller than at SATURNE II energies, where it has been estimated to be less than 0.05 mb. This is much smaller than the statistical error in the present experiment.

The neutron detection efficiencies of about 2% for all detectors are practically constant with energy. The efficiencies were determined with respect to a calibrated ionization chamber in front of the production target.

The counter array used provides very good stability of the detection efficiency. Note that the results depend neither on the absolute efficiencies of S_i and T_j, nor on their ratio (Eq.(6.3)). The small detection efficiencies decrease the probability for a converted neutron to be accompanied by another quasi-simultaneous converted neutron in the same detector. The "simultaneous" detection is to be understood within the resolution time of a plastic scintillation counter (20 nsec). This probability was estimated from results obtained with different neutron beam intensities and radiator thicknesses [3,4]. For the same neutron fluxes, it increases quadratically with increasing $\eta_{S,T}$. For high counter efficiencies (namely for pp transmission experiments) it represents the dominant source of systematic errors. At SATURNE II the neutron counter efficiences were of the same order, the neutron beam intensity was around

7.10^7/spill (hundred times more) and the spill length was compatible with that of the Synchrophasotron. The simultaneous conversion probability has been found to be always smaller than 10^{-4}, corresponding to a maximum systematic error of ± 0.25 mb at Saclay. It was estimated to be negligible in the present experiment.

Possible misalignment of the detector components or the entire detectors provide left-right (up-down) instrumental asymmetries. The asymmetries in each S_i and T_j detector will depend on the transverse beam polarization components (P_{Bn} and P_{Bs}) only. For T_j detectors they are practically independent of the target polarization [3,18]. This asymmetry $\epsilon_{Bn}(instrum)$ may be of the same order or larger than the transmission effects, even for a small counter and radiator misalignment. The $\epsilon_{Bn}(instrum)$ provides the same contributions to each pair of measurements in Eqs.(2.7ab) and (2.7c,d) and it cancels out when taking the simple average of results in Eq.(6.4). Since the present experiment uses almost longitudinal beam, the displacement effects for $\Delta\sigma_L$ can be neglected.

The distribution of results from independent measurements for the same sign of the target polarization show that fluctuations were about 1.005 times larger than expected from statistics alone. We have added quadratically an error of $\pm 0.5\%$ for random-like instrumental effects.

Table 4

Existing data for np differential cross sections and predictions for $A_{ookk}(np)$ close to 180° CM at several energies.

$T_{kin}(n)$ (GeV)	$(d\sigma/d\Omega)(180°)$ (mb)	A_{ookk} $170°CM$	A_{ookk} $175°CM$	A_{ookk} $180°CM$
0.80	8.14 ± 0.19	-0.549	-0.864	-0.911
0.90	8.70 ± 0.62	-0.472	-0.840	-0.899
1.00	8.70 ± 0.27	-0.409	-0.828	-0.897
1.10	9.11 ± 0.27	-0.360	-0.825	-0.903
1.20	7.32 ± 0.25	-0.329	-0.832	-0.916
1.30	4.30 ± 0.35	-0.317	-0.846	-0.933
2.50	3.00 ± 0.30			
4.15	2.26 ± 0.24			

A possible inefficiency of the protection against charged particles (veto counters $S3A$ and $T3A$) may exist. Charged particles in the neutron beam are produced mainly in beam collimators, in CH_2 radiators of all S_i and T_j detectors, and in the target. Only a small fraction of the forward protons is polarized. They are produced in the polarized target by elastic scattering of polarized neutrons on free polarized

protons close to $\theta_{CM} = 180^o$. For the longitudinally polarized beam and target one obtains a contribution from the spin correlation parameter $A_{ookk}(np)$, which is included in the counting rate asymmetry for the observable $\Delta\sigma_L$. The A_{ookk} spin correlation has been measured at 1.10 GeV where its value at 178.7° CM reaches -0.53 ± 0.01 [29]. This observable shows a rapid decrease towards large negative values as a function of scattering angle. This could be seen in Table 4 where predictions for $A_{ookk}(np)$ close to 180° CM [30] together with measured np differential cross sections in the backward direction are listed.

In the present experiment at 1.19 GeV within the labotarory solid angle $\Delta\Omega(lab) = 3.44 \times 10^{-4} sr$ (i.e. $\Delta\Omega(CM) = 2.27 \times 10^{-3} sr$) and with the flux of 10^5 neutrons/spill, one obtains less than 1 scatter/spill. This corresponds to an additional asymmetry of 10^{-4} for completely inefficient veto counters. From Table 4 it follows that the spin correlation parameter contribution $A_{ookk}(np)$ moves $-\Delta\sigma_L(np)$ towards negative values. Since the efficiencies of veto counters are better than 98% the additional asymmetry will decrease to 2.10^{-6} and may provide a ±0.1% systematic error. The $A_{ookk}(180^o)CM$ observable represents one of parameters which determine the real parts of scattering amplitudes for the isospin $I = 0$ state. A measurement of this observable at 180° CM is foreseen in the future.

Table 5

Transmission measurements for different MPT configurations.

MPT configuration	Transmission ratio
MPT absent	1.000
MPT solenoid istalled only	0.994
MPT without the propanediol sample	0.936
MPT operationnel	0.729

Other checks were performed in order to estimate the target effects. Measurements were carried out with an empty polarized target, with the target removed from the solenoid and without any target element in the neutron beam line. Results of these tests are listed in Table 5. All transmission ratio results are in excellent agreement with calculated values.

In Table 6 is given a summary of the maximal contributions to $\Delta\sigma_L(np)$ from different sources of systematic uncertainties.

Table 6

Summary of systematic uncertainties.

Origin of the uncertainty	Contribution $\pm$ to $\Delta\sigma_L(np)$ (%)
Beam polarization	2.3
Target polarization	3.0
Number of polarized target H-atoms	3.1
Neutron spin rotator	1.1
Polarization of other atoms	0.3
Inefficiencies of veto counters	0.1
Random-like instrumental effects	0.5

The total systematic error is then $\pm 5\%$ of the measured value. The absolute error of ± 0.05 mb due to the extrapolation towards zero solid angle is to be added.

7. RESULTS AND DISCUSSION

All combinations of the two monitors $S_{1,2}$ and three transmission detectors $T_{1,2,3}$ counting rates were taken into account. They provided a check of the compatibility of the results. The final results for this experiment were deduced from measured rates $\sum_i S_i$ and $\sum_j T_j$ for corresponding beam and target polarization configurations. They are listed in Table 7. The errors of the present results contain statistical and systematic errors added in quadrature. Results are shown in Fig. 3 together with existing data [3,4,6,8,9] measured with free polarized neutrons. All data smoothly connect in the entire energy region. The solid curve was calculated by the energy dependent phase shift analysis [30] where the present results were not introduced. We observe a fast decrease in the $-\Delta\sigma_L(np)$ energy dependence. This seems to be in disagreement with the PSA predictions, but no extrapolation is allowed out of the region of existing data.

In Fig. 4 the fit to data above 0.4 GeV (curve 1) is compared with the difference between $-\Delta\sigma_L(dp)$ and $-\Delta\sigma_L(pp)$ results obtained at the ANL-ZGS [13]. We observe a good agreement above 1 GeV and a confirmation of the $-\Delta\sigma_L(np)$ energy dependence, discussed above.

The similar quantity in pp transmission, $\Delta\sigma_L(pp)$, also decreases with energy [2] and tends to zero. This is in agreement with the prediction of a nonperturbative QCD model for spin effects, treated in ref.[31]. The model predicts that the quark interaction induced by strong fluctuations of vacuum gluon fields, i.e. instantons

[32], provides the large contribution to the $\Delta\sigma_L$ observable [33]. Important features of this interaction are its spin and flavor dependence. The interaction cannot vanish only for the quarks which have the same helicity but a different flavor. The maximal instanton contribution to the $-\Delta\sigma_L(np)$ is shown in Fig. 4 by the dot-dashed curve (2). Two minima were predicted for instanton-induced contribution : one close the two-pion production threshold (a), second one at the $(2\pi + \eta)$ threshold (b). The model can explain qualitatively the observed $\Delta\sigma_L$ energy dependence for np as well as for pp transmission.

It will be very interesting to measure the total cross section difference $\Delta\sigma_T(np)$, using the tranversely polarized beam and target. This quantity may show a different behavior at high energies, according to a prediction of this model.

The lowest lying exotic quark configurations in the isospin state $I = 1$ and the spin-singlet state $^1S_0$ with the mass of 2.7 GeV ($T_{kin}(p) = 2.1$ GeV) was predicted by Lomon, LaFrance and Gonzalez [34-38]. The authors used the Cloudy Bag Model and an R-matrix connection to long range meson exchange forces. Their prediction is in qualitative agreement with Resonating Group Method calculations for constituent quark models (CQM), as predicted by Wong [39] for the relativistic CQM, and by Kalashnikova, Narodetskii and Simonov [40] for the non-relativistic CQM.

A resonance-like structure has been suggested by the energy dependence of the $\Delta\sigma_L(pp)$ [2,41], as well as by the measurement of the spin correlation parameter $A_{oonn}(pp)$ at $90°CM$ [42]. Other indications can be found in refs.[43-48]. The present data allow no conclusions yet and new measurements with smaller steps in energy throughout the region from 1.5 to 4.0 GeV are highly desirable.

Using the known $\Delta\sigma_L(pp)$ data one deduces $\Delta\sigma_L$ values for $I = 0$ from :

$$\Delta\sigma_L(I = 0) = 2\Delta\sigma_L(np) - \Delta\sigma_L(pp). \qquad (7.1)$$

These data will have roughly two times larger errors than np data. In order to deduce $\Delta\sigma_L(I = 0)$ values from the present measurements, the averaged values of the $\Delta\sigma_L(pp)$ data measured at SATURNE II and at the ANL-ZGS were used (see ref.[2] and references therein). The results are given in Table 7 and plotted in Fig. 5, together with the PSA predictions from [30] and the values deduced from PSI, LAMPF, ANL-ZGS and Saclay np measurements.

The $-\Delta\sigma_L(I = 0)$ value sharply increase towards low energy (at 66 MeV $-\Delta\sigma_L(I = 0) = (88.6 \pm 4.0)$ mb). At high energies we observe an unexpected although well pronounced maximum somewhere above 1.5 GeV, followed by a rapid decrease with increasing energy. It means that $-2\Delta\sigma_L(np)$ decreases faster then $-\Delta\sigma_L(pp)$ in this energy range. This behaviour is also in qualitative agreement with

the instanton model. It supports more strongly the prediction of ref.[49], concerning a position ot the lowest lying exotic quark configuration for isospin $I = 0$ in the spin-triplet wave $^3S_1$ at a mass 2.63 GeV ($T_{kin}(n) = 1.8$ GeV). In the $\Delta\sigma_L(I = 0)$ the spin-singet partial wave $^1S_0$ ($I = 1$) is absent and the $^3S_1$ wave ($I = 0$) may be predominant. To confirm this observation a measurement of $\Delta\sigma_T(np)$ is needed in order to deduce $\Delta\sigma_T(I = 0)$. In the last quantity the uncoupled spin-triplet is absent and the coupled spin-triplet amplitude is expected to be less diluted.

Table 7

-$\Delta\sigma_L(np)$, -$\Delta\sigma_L(pp)$ and -$\Delta\sigma_L(I = 0)$ data.

$T_{kin}(n)$ (GeV)	-$\Delta\sigma_L(np)$ (mb)	-$\Delta\sigma_L(pp)$ (mb)	-$\Delta\sigma_L(I = 0)$ (mb)
1.19	7.10 ± 3.70	9.98 ± 0.25	4.22 ± 7.40
2.49	-0.85 ± 1.32	2.02 ± 0.29	-3.72 ± 2.64
3.65	0.30 ± 0.84	1.74 ± 0.04	-1.14 ± 1.68

8. CONCLUSIONS

The present results increase the energy range of existing $\Delta\sigma_L(np)$ data up to 3.66 GeV. The Dubna results connect smoothly with the Saclay free np measurements and are in excellent agreement with the pn quasielastic ANL-ZGS data. They are compared with existing models and with the presictions of the phase shift analysis. Using the present np results and the existing pp data measured at SATURNE II and at ANL-ZGS, the $\Delta\sigma_L$ values for the isospin state $I = 0$ were obtained. They show a well pronounced sharp maximum above 1.5 GeV. Our results will improve spin-dependent dispersion-relation calculations as well as the existing PSA solutions. The data can also be used to check theoretical models.

ACKNOWLEDGEMENTS

We acknowledge support for this work from J. Arvieux, A.M. Baldin, P. Borgeaud, F. Bradamante, V.P. Dzhelepov, J.Haïssinski, I.M. Karnaukhov, Ph.Leconte, Yu.C. Oganesian, V.A. Matveev, B.Peyaud, V.S. Rumyantsev, N.A. Russakovich, I.A.Savin, A.N. Sissakian, J.J. de Swart and H.Walter. Discussions with J. Bystricky, P. Chaumette, J. Derégel, A.E. Dorokhov, M.Finger, M.Giorgi, R.Hess, Z.Janout, Yu.F. Kisselev, R. Kunne, C. Lechanoine-Leluc, S.Mango, S.B. Neganov, S. Pospíšil, D.Rapin, M.P.Rekalo, I.I. Strakovsky, I.Wilhelm, and C.Wilkin have solved several problems. We thank the accelerator crew and N.N. Agapov with the staff of

the liquid helium plant as well as the LNP and LHE JINR workshop staff for efficient help. The exploitation of the polarized target owes a lot to A.V.Gevchuk and R.L.Khamidulin. We acknowledge contributions of T.B. Ivashkevich, Z.P. Motina, V.M. Zhabitsky and P.I. Zarubin to organization of the experiment. This work was partly supported by the International Association for the Promotion of Cooperation with Scientists from the Independent States of the Former Soviet Union (INTAS) grant No 93-3315, by the Russian Foundation for Basic Research grants RFBR-93-02-03961, RFBR-93-02-16715 and RFBR-95-02-05807, by the International Science Foundation and Russian Government grant No. JWH 100, and by the US Department of Energy Contract No. W-31-109-ENG-38.

REFERENCES

[1] I.B. Issinsky, A.D. Kirillov, A.D. Kovalenko and P.A. Rukoyatkin, Acta Physica Polonica **B25** (1994) 673

[2] C. Lechanoine-Leluc and F.Lehar, Rev.Mod.Phys. **65** (1993) 47

[3] F.Lehar, A. de Lesquen, L. van Rossum, P.Chaumette, J.Derégel, J.Fabre, M. de Mali, J.M.Fontaine, D.Legrand, F.Perrot, J.Ball, C.D.Lac, P.Bach, G.Gaillard, R.Hess, Ph.Sormani, V.Ghazikhanian, C.A.Whitten, R.Peschina, E.Rössle, Phys.Lett. **189B** (1987) 241

[4] J.M. Fontaine, F. Perrot-Kunne, J. Bystricky, J. Derégel, F.Lehar, A. de Lesquen, M. de Mali, L. van Rossum, J. Ball, Ph. Chesny, C.D. Lac, J.L. Sans, J.P. Goudour, P. Bach, G. Gaillard, R. Hess, R. Kunne, D. Rapin, Ph. Sormani, R. Binz, A. Klett, R. Peschina, E. Rössle, H. Schmitt, Nucl.Phys. **B358** (1991) 297

[5] J.Ball, Ph.Chesny, M.Combet, J.M.Fontaine, R.Kunne, M.C.Lemaire, J.L.Sans, J.Bystricky, F.Lehar, A. de Lesquen, M. de Mali, F.Perrot-Kunne, Ph.Demierre, G.Gaillard, R.Hess, D.Rapin, L.S.Barabash, Z.Janout, B.A.Khachaturov, Yu.A.Usov, D.Lopiano, H.Spinka, R.Binz, A.Klett, E.Rössle, H.Schmitt, Zeit.Phys. **C61** (1994) 53

[6] R.Binz, B. van den Brandt, R.Büchle, M.Daum, Ph.Demierre, J.Franz, G.Gaillard, N.Hamann, R.Hess, J.A.Konter, F.Lehar, C.Lechanoine-Leluc, S.Mango, R.Peschina, F.Perrot-Kunne, D.Rapin, E.Rössle, P.A.Schmelzbach, H.Schmitt and R.Todenhagen, Nucl.Phys. **A533** (1991) 601

[7] R.Binz, R.Büchle, M.Daum, J.Franz, G.Gaillard, N.Hamann, R.Hess, S.Jaccard, F.Lehar, C.Lechanoine-Leluc, A.C.Letestu, R.Peschina, D.Rapin, E.Rössle, P.A.Schmelzbach, H.Schmitt, R.Todenhagen, and H.L.Woolverton, Phys.Lett. **B231** (1989) 323

[8] M. Beddo, G. Burleson, J.A. Faucett, S. Gardiner, G.Kyle, R.Garnett, D.P.Grosnick, D. Hill, K.F. Johnson, D.Lopiano, Y.Ohashi, T.Shima, H. Spinka, R. Stanek, D. Underwood, A. Yokosawa, G.Glass, R.Kenefick, S.Nath, L.Northcliffe, J.J.Jarmer, S.Penttila, R.H.Jeppesen, G.Trippard, M.Devereux and P.Kroll, Phys.Lett. **258B** (1991) 24

[9] P.Hafner, C.Brogli-Gysin, J.Campbell, D.Fritschi, J.Götz, M.Hammans, R.Henneck, J.Jourdan, G.Masson, L.M.Quin, S.Robinson, I.Sick, M.Tucillo, J.A.Konter, S.Mango and B. van den Brandt, Nucl.Phys. **A548** (1992) 29

[10] W.S.Wilburn, C.R.Gould, D.G.Haase, P.R.Huffman, C.D.Keith, J.E.Koster, N.R.Roberson and W.Tornow, Phys.Rev.Lett. **71** (1993) 1982

[11] W.S.Wilburn, C.R.Gould, D.G.Haase, P.R.Huffman, C.D.Keith, N.R.Roberson and W.Tornow, Phys.Rev. **C52** (1995) 2353

[12] J. Brož, J. Černý, Z. Doležal, G.M. Gurevich, M. Jirásek,. P. Kubík, A.A. Lukhanin, J. Švejda, I. Wilhelm, N.S. Borisov, Yu.M. Kazarinov, B.A. Khachaturov, E.S. Kuzmin, V.N. Matafonov, A.B. Neganov, I.L. Pisarev, Yu.A. Plis, Yu.A.Usov, M.Rotter and B.Sedlák, Zeit.Phys. A, to be published 1996

[13] I.P.Auer, W.R.Ditzler, D.Hill, H.Spinka, N.Tamura, G.Theodosiou, K.Toshioka, D.Underwood, R.Wagner, and A.Yokosawa, Phys.Rev.Lett. **46** (1981) 1177

[14] W.Grein and P.Kroll, Nucl.Phys. **A377** (1982) 505

[15] J.Bystricky, F.Lehar and P.Winternitz, J.Physique (Paris) **39** (1978) 1

[16] S.M.Bilenky and R.M.Ryndin, Phys.Lett. 6 (1963) 217
[17] R.J.N.Phillips, Nucl.Phys. 43 (1963) 413
[18] F.Perrot, H. Azaiez, J.Ball, J. Bystricky, P. Chaumette, Ph. Chesny, J. Derégel, J. Fabre, J.M. Fontaine, J. Gosset, F. Lehar, W.R.Leo, A. de Lesquen, C.R. Newsom, Y.Onel, A.Penzo, L. van Rossum, T. Siemiarczuk, J. Vrzal, C.A. Whitten and J. Yonnet, Nucl.Phys. **B278** (1986) 881
[19] V.G. Ableev, S. Dzhemukhadze, V.P. Ershov, V.V. Fimushkin, B.Kühn, M.V. Kulikov, A.A. Nomofilov, L.Penchev, Yu.K. Pilipenko, N.M. Piskunov, V.I.Sharov, V.B. Shutov, I.M. Sitnik, E.A. Strokovsky, L.N. Strunov, S.A.Zaporozhets, B.Naumann, L.Naumann and S.Tesch, Nucl.Instrum.Methods **A306** (1991) 73
[20] V.Ghazikhanian, B.Aas, D.Adams, E.Bleszynski, M.Bleszynski, J.Bystricky, G.J.Igo, T.Jaroszewicz, F.Sperisen, C.A.Whitten, P.Chaumette, J.Derégel, J.Fabre, F.Lehar, A. de Lesquen, L. van Rossum, J.Arvieux, J.Ball, A.Boudard and F.Perrot, Phys.Rev. **C43** (1991) 1532
[21] J.Bystricky, F.Lehar, A. de Lesquen, A.Penzo, L. van Rossum. J.M.Fontaine, F.Perrot, G.Leleux and A.Nakach : Nucl.Instrum.Methods **A234** (1985) 412
[22 J.Ball, Ph.Chesny, M.Combet, J.M.Fontaine, R.Kunne, M.C.Lemaire, J.L.Sans, J.Bystricky, C.D.Lac, F.Lehar, A. de Lesquen, M. de Mali, F.Perrot-Kunne, L. van Rossum, P.Bach, Ph.Demierre, G.Gaillard, R.Hess, D.Rapin, Ph.Sormani, J.P.Goudour, R.Binz, A.Klett, E.Rössle, H.Schmitt, L.S.Barabash, Z.Janout, B.A.Khachaturov, Yu.A.Usov, D.Lopiano, H.Spinka, Nucl.Phys. **A559** (1993) 477
[23] A.N. Prokofiev, V.V. Vikhrov, A.A. Zhdanov, L.S. Azhgirey, N.M. Piskunov, G.D. Stoletov, F.Lehar, Polarimeter for the Deuteron Beam at the JINR Synchrophasotron, Proceedings of the International Seminar "DEUTERON 95", Dubna 1995, to be published
[24] J.Ball, Ph.Chesny, M.Combet, J.M.Fontaine, C.D.Lac, J.L.Sans, P.Chaumette, H.Desportes, J.Derégel, G.Durand, J.Fabre, L. van Rossum, D.Hill : Dilution Refrigerator and Solenoid for the FERMILAB Spin Physics Facility, 8th International Symposium on High Energy Spin Physics, Minneapolis, Minnesota, USA, September 12-17, 1988 AIP Conference Proceedings No. 187, N.Y. 1989, Particles and Fields Series 37, Vol. II, 1331 and 1334
[25] D.L.Adams, N.Akchurin, N.I.Belikov, J.Bystricky, P.Chaumette, M.D.Corcoran, J.D.Cossairt, J.Cranshaw, J.Derégel, A.A.Derevschikov, G.Durand, H.En'yo, J.Fabre, K.Fukuda, H.Funahashi, Y.Goto, O.A.Grachov, D.P.Grosnick, D.A.Hill, K.Imai, Y.Itow, K.Iwatani, K.W.Krueger, K.Kuroda, M.Laghai, F.Lehar, A. de Lesquen, D.Lopiano, F.C.Luehring, A.Maki, S.Makino, A. Masaike, Yu.A. Matulenko, A.P. Meshanin, A. Michalowicz, D.H.Miller, K.Miyake, T.Nagamine, F. Nessi-Tedaldi, M.Nessi, C.Nguyen, S.B.Nurushev, Y.Ohashi, Y.Onel, D.I.Patalakha, G.Pauletta, A.Penzo, A.L.Read, J.B.Roberts, L. van Rossum, V.L.Rykov, N.Saito, G.Salvato, P.Shiavon, J.Shepard, J.Skeens, V.L.Solovyanov, H.Spinka, R.Takashima, F.Takeutchi, N.Tamura, N.Tanaka, D.G.Underwood, A.N.Vasiliev, A.Villari, J.L.White, S.Yamashita, A.Yokosawa, T.Yoshida and A.Zanetti, Phys.Lett. **261B** (1991) 197

[26] F. Lehar, B. Adiasevich, V.P. Androsov, N. Angelov, N. Anischenko, V. Antonenko, J. Ball, V.G. Baryshevsky, N.A. Bazhanov, A.A. Belyaev, B. Benda, V. Bodyagin, N. Borisov, Yu. Borzunov, F. Bradamante, E. Bunyatova, V. Burinov, E. Chernykh, M. Combet, A. Datskov, G. Durand, A.P. Dzyubak, J.M. Fontaine, V.A. Get'man, M. Giorgi, L. Golovanov, V. Grebenyuk, D. Grosnick, G. Gurevich, T. Hasegawa, D. Hill, N. Horikawa, G. Igo, Z. Janout, V.A. Kalinnikov, I.M. Karnaukhov, T. Kasprzyk, B.A. Khachaturov, A. Kirillov, Yu. Kisselev, E.S. Kousmine, A. Kovalenko, A.I. Kovaljov, V.P. Ladygin, A. Lazarev, Ph. Leconte, A. de Lesquen, A.A. Lukhanin, S. Mango, A. Martin, V.N. Matafonov, E. Matyushevsky, S. Mironov, A. Neganov, B.S. Neganov, A. Nomofilov, V. Perelygin, Yu. Plis, Yu. Pilipenko, I.L. Pisarev, N. Piskunov, Yu. Polunin, Yu.P. Popkov, A.A. Popov, A.N. Prokofiev, M.P. Rekalo, P. Rukoyatkin, J.L.Sans, M.G. Sapozhnikov, V. Sharov, S. Shilov, Yu. Shishov, I.M. Sitnik, P.V. Sorokin, H.Spinka, E.A. Sporov, L.N. Strunov, A. Svetov, J.J. de Swart, Yu.P. Telegin, I. Tolmashov, S. Trentalange, A. Tsvinev, Yu.A. Usov, V.V. Vikhrov, C. Whitten, S. Zaporozhets, A. Zarubin, A.A.Zhdanov, L. Zolin,
Nucl.Instrum.Methods **A356** (1995) 58

[27] E.I.Bunyatova, R.M.Galimov, S.A.Luchkina, "Investigation of Stable Paramagnetic HMBA Complex in Different Solvents", Preprint JINR 12-82-732, Dubna 1982

[28] R.Bernard, P.Chaumette, P.Chesny, J.Derégel, R.Duthil, J.Fabre, C.Lesmond, G.Seite, J.Ball, T.O.Niinikoski, and M.Rieubland,
Nucl.Instrum.Methods **A249** (1986) 176

[29] R.Binz, PhD Thesis : Untersuchung der spinabhängigen Neutron-Proton Wechselwirkung im Energiebereich von 150 bis 1100 MeV, University of Freiburg im Breisgau 1991.

[30] R.A. Arndt, I.I. Strakovsky, and R.L. Workman, Phys.Rev. C50 (1994) 2731

[31] A.E.Dorokhov, N.I.Kochelev and Yu.A.Zubov, Int.J.Mod.Phys. A8 (1993) 603

[32] G.'t Hooft, Phys.Rev. D14 (1976) 3432

[33] N.I.Kochelev, 3rd International Symposium "DUBNA DEUTERON-95", Dubna, to be published

[34] E.L.Lomon, Colloque de Physique (France) 46 (1985) C2-329

[35] P.LaFrance and E.L.Lomon, Phys.Rev. D34 (1986) 1341

[36] P.Gonzales, P.LaFrance and E.L.Lomon, Phys.Rev. D35 (1987) 2142

[37] E.L.Lomon, 8th International Symposium on High Energy Spin Physics, Minneapolis, Minnesota, USA, September 12-17, 1988 AIP Conference Proceedings No. 187, N.Y. 1989 Particles and Fields Series 37, Vol. I, p.655

[38] E.L. Lomon, Colloque de Physique (France) 51 (1990) C6-363

[39] C.W.Wong, Prog. in Part. and Nucl.Phys. 8 (1982) 223

[40] Yu.S.Kalashnikova, I.M.Narodeckii and Yu.A.Simonov, Yad.Fiz. 46 (1987) 1181, transl. Sov.J.Nucl.Phys. 46 (1987) 689

[41] I.P.Auer, E.Colton, W.R.Ditzler, H.Halpern, D.Hill, R.C.Miller, H.Spinka, N.Tamura, J.-J.Tavernier, G.Theodosiou, K.Toshioka, D.Underwood, R.Wagner, and A.Yokosawa, Phys.Rev.Lett. 62 (1989) 2649

[42] J.Ball, P.A. Chamouard, M.Combet, J.M.Fontaine, R.Kunne, J.M.Lagniel, J.L.Lemaire, G.Milleret, J.L.Sans, J.Bystricky, F.Lehar, A. de Lesquen, M. de Mali, Ph.Demierre, R.Hess, Z.F.Janout, E.L.Lomon, D.Rapin, B.Vuaridel, L.S.Barabash, Z.Janout, V.A.Kalinnikov, Yu.M.Kazarinov, B.A.Khachaturov, V.N.Matafonov, I.L. Pisarev, A.A. Popov, Yu.A. Usov, M.Beddo, D. Grosnick, T. Kasprzyk, D.Lopiano, H.Spinka, A. Boutefnouchet, V. Ghazikhanian, C.A.Whitten, Phys.Lett. **B320** (1994) 206

[43] D.V. Bugg, D.C. Salter, G.H. Stafford, R.F. George, K.F. Riley, R.J. Tapper, Phys.Rev. **146** (1966) 980

[44] H.Spinka, E. Colton, W.R.Ditzler, H.Halpern, K.Imai, R. Stanek, N. Tamura, G.Theodosiou, K. Toshioka, D. Underwood, R.Wagner, Y. Watanabe, A. Yokosawa, G.R. Burleson, W.B. Cottingame, S.J.Greene, S.Stuart, J.J.Jarmer, Nucl.Instrum.Methods **211** (1983) 239

[45] C.D.Lac, J.Ball, J.Bystricky, J.Derégel, F.Lehar, A. de Lesquen, L. van Rossum, J.M.Fontaine, F.Perrot and P.Winternitz, J.Phys. (France) **51** (1990) 2689

[46] R.Bertini, J.Arvieux, M.Boivin, J.M.Durand, F.Soga, E.Descroix, J.Y.Grossiord, A.Guichard, J.R.Pizzi, Th.Hennino and L.Antonuk, Phys.Lett. **162B** (1985) 77

[47] R.Bertini, G.Roy, J.M.Durand, J.Arvieux, M.Boivin, A.Boudard, C.Kerboul, J.Yonnet, M.Bedjidian, J.Y.Grossiord, A.Guichard, J.R.Pizzi, Th.Hennino and L.Antonuk, Phys.Lett. **203B** (1988) 18

[48] J.Yonnet, R.Abegg, M.Boivin, A.Boudard, G.Bruge, P.Couvert, G.Gaillard, M.Garcon, L.G.Greeniaus, D.A.Hutcheon, C.Kerboul and B.Mayer, Nucl.Phys. **A562** (1993) 352

[49] P. LaFrance and E.L.Lomon, Proceedings of International Conference on "Mesons and Nuclei at Intermediate Energies", Dubna, 3-7 Mai 1994, Editors M.Kh.Khankhasayev and Zh.B.Kurmanov, World Scientific, Singapore 1995-XV, p.97

[50] J.Bystricky, C.Lechanoine-Leluc and F.Lehar, J.Physique (France) **51** (1990) 2747

[51] J.Bystricky, C.Lechanoine-Leluc, F.Lehar, J.Physique (Paris) 48 (1987) 199

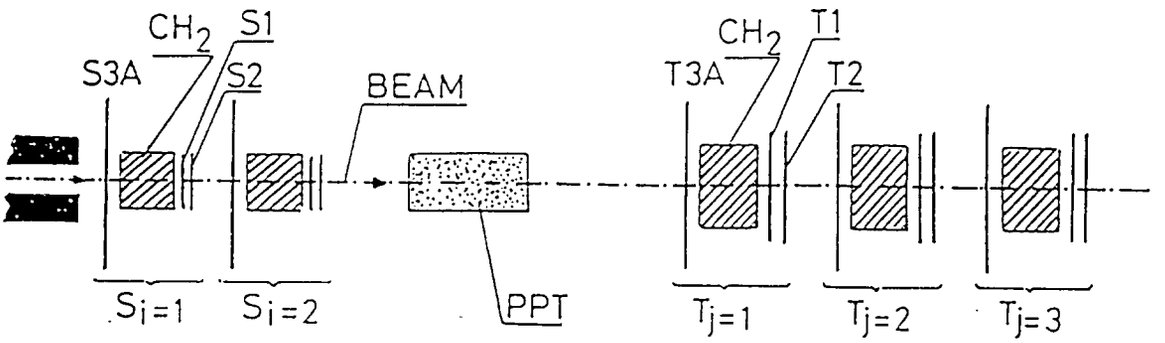

Fig. 1 Experimental set-up for the $\Delta\sigma_L(np)$ measurements. $S1$, $S2$, $S3A$, $T1$, $T2$ and $T3A$ are scintillation counters, and CH_2 are radiators.

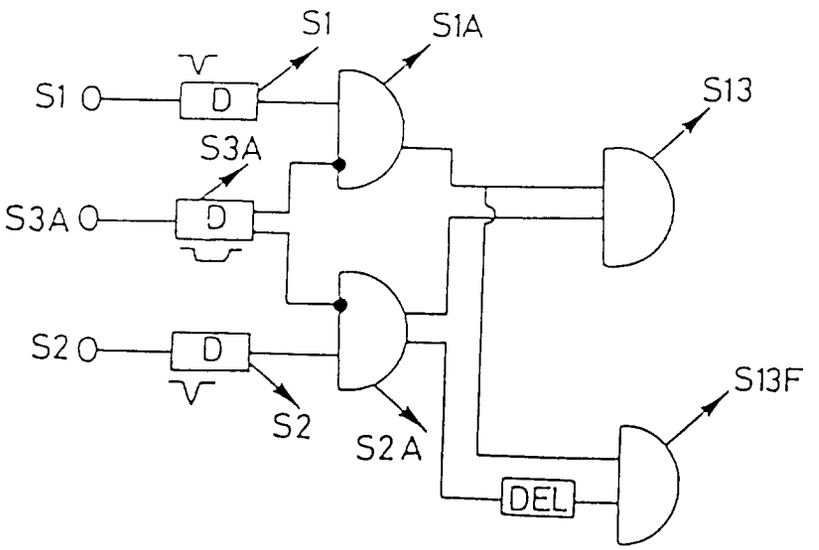

Fig. 2 Electronic diagram of the monitor detectors. D are discriminators, and arrows denote the scalers.

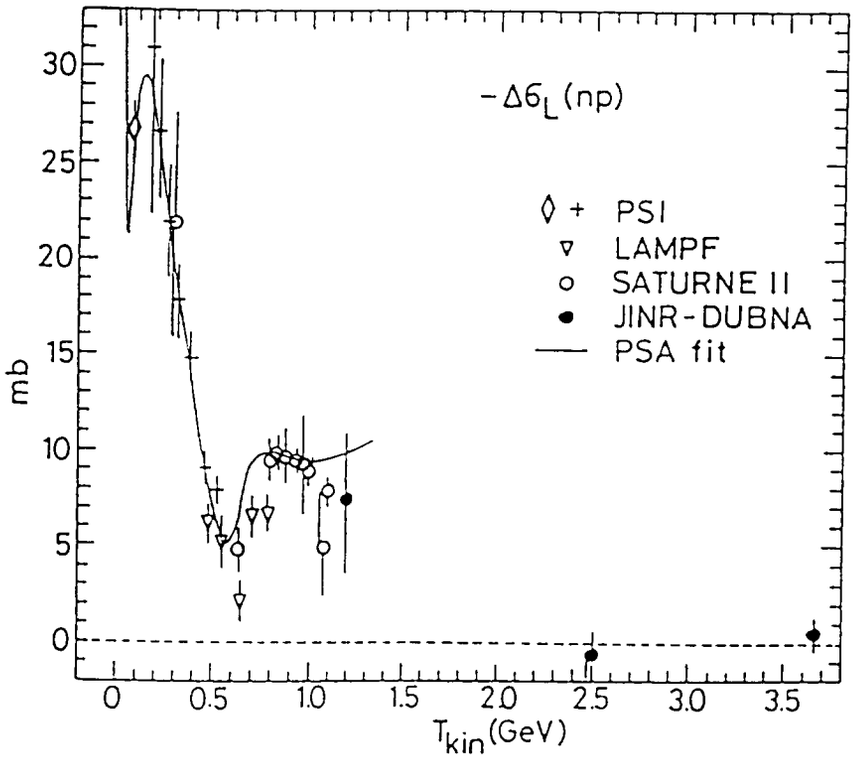

Fig. 3 Energy dependence of $\Delta\sigma_L(np)$. Meaning of the symbols : • ..... present experiment, diamond ..... PSI, ref.[9], + ... PSI, ref.[6], ▽ ..... LAMPF, ref.[8], o ..... SATURNE II, refs.[3,4], solid line ..... PSA, ref.[30].

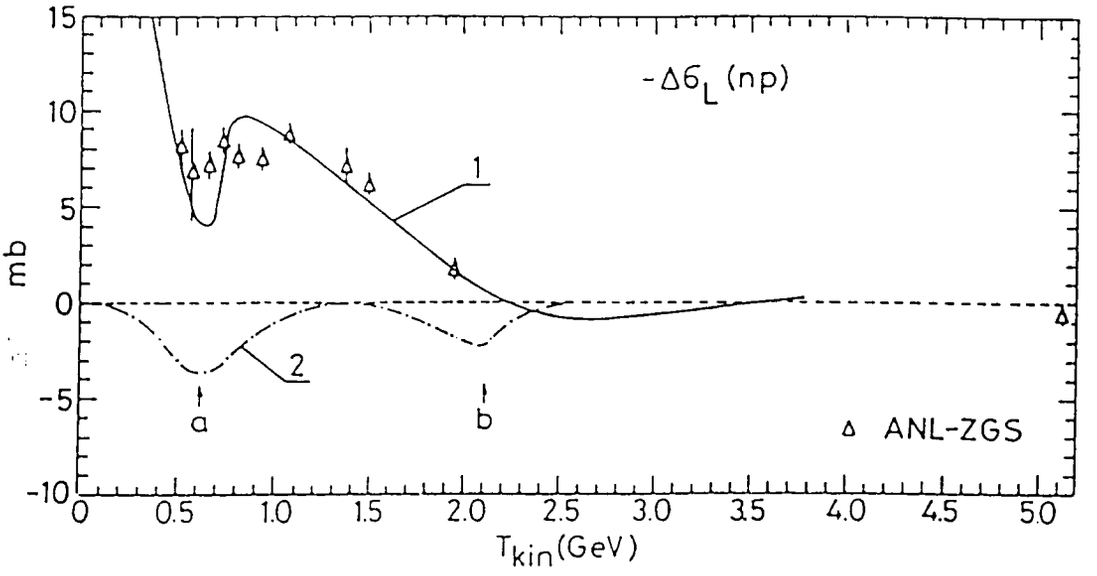

Fig. 4 Fit to the existing np data (solid curve 1) compared with ANL-ZGS data from ref.[13] (Δ). The maximal instanton contribution to the $-\Delta\sigma_L(np)$ is shown by the dot-dashed curve 2. Two minima were predicted for instanton-induced contribution [33] : one close the two-pion production threshold (a), second one at the $(2\pi + \eta)$ threshold (b).

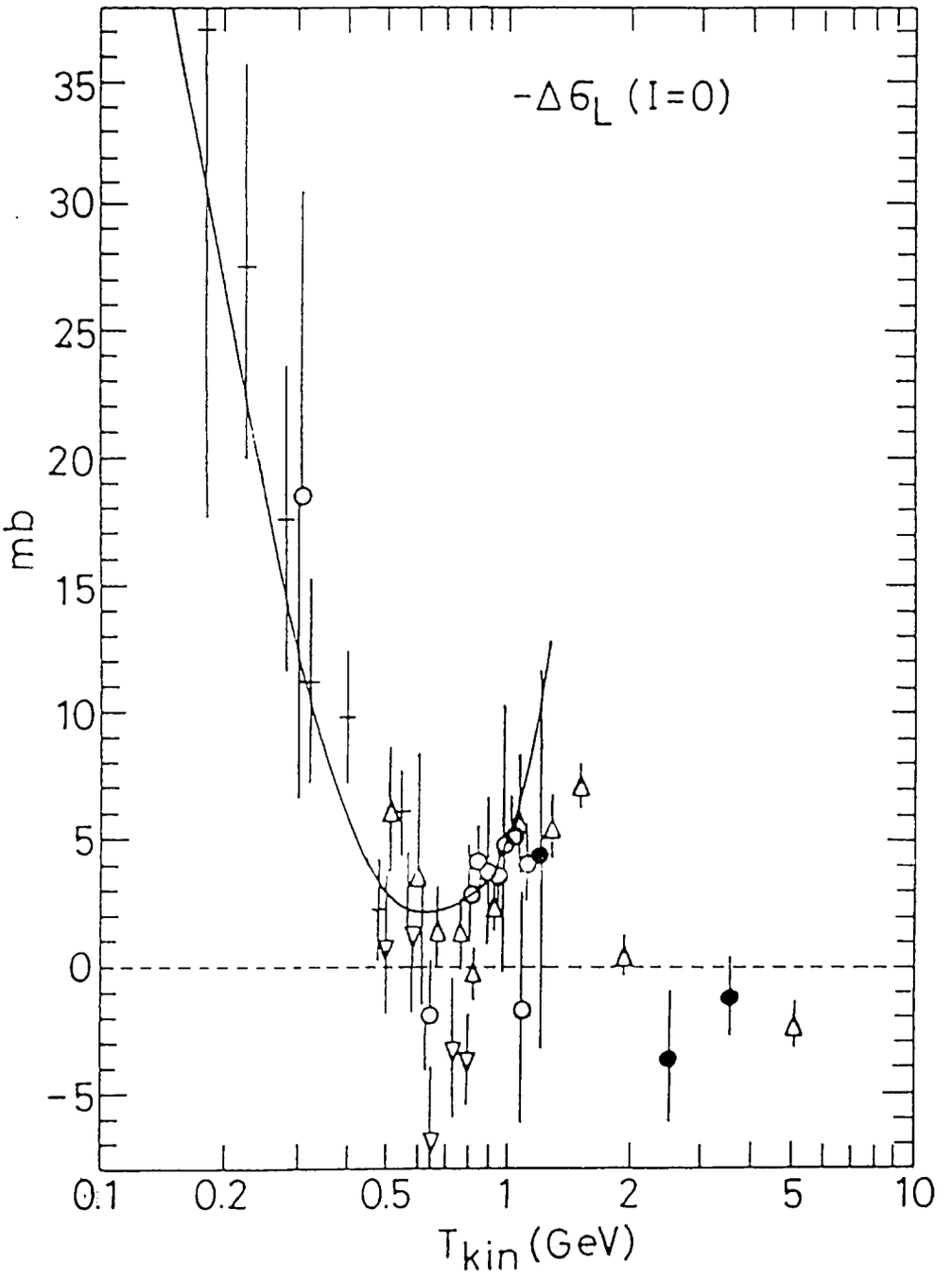

Fig. 5 Energy dependence of $\Delta\sigma_L(I=0)$. The *np* data plotted in Figs. 3 and 4 were used (the present symbols have the same meaning). The *pp* data were calculated from the Saclay-Geneva PSA [50,51] for *np* results from refs.[3,4,6,8]. ANL-ZGS $I=0$ data are given by authors of ref.[13]. At 1.19 and 2.49 GeV *pp* data were taken as average values from ANL-ZGS and SATURNE II measurements [3,4,13]. At 3.65 GeV interpolated *pp* values from ANL-ZGS were used.